

PAPER

Transport through the network of topological channels in HgTe based quantum well

To cite this article: G M Gusev *et al* 2022 *2D Mater.* **9** 015021

View the [article online](#) for updates and enhancements.


You may also like

- [Utility of an Empirical Method of Modeling Combined Zero Gap/Attached Electrode Membrane ChlorAlkali Cells](#)
Clifford W. Walton and Ralph E. White
- [Membrane-Based Zero Gap CO₂ Electrolyzer with Au Cathode Prepared By Electrodeposition](#)
Junhyeong Kim, Wenwu Guo, Gyeong Ho Han et al.
- [Transport property of the organic conductor -\(BEDT-STF\)₂I₃ in the magnetic field](#)
M Sato, S Sugawara, N Tajima et al.



PAPER

Transport through the network of topological channels in HgTe based quantum well

RECEIVED
25 August 2021REVISED
20 October 2021ACCEPTED FOR PUBLICATION
31 October 2021PUBLISHED
30 November 2021G M Gusev^{1,*} , Z D Kvon^{2,3}, D A Kozlov², E B Olshanetsky², M V Entin² and N N Mikhailov²¹ Instituto de Física da Universidade de São Paulo, 135960-170 São Paulo, SP, Brazil² Institute of Semiconductor Physics, Novosibirsk 630090, Russia³ Novosibirsk State University, Novosibirsk 630090, Russia

* Author to whom any correspondence should be addressed.

E-mail: gusev@if.usp.br**Keywords:** topological insulator, two-dimensional systems, Dirac fermions, topological network**Abstract**

Topological insulators (TIs) represent a new quantum state of matter which is characterized by edge or surface states and an insulating band gap in the bulk. In a two-dimensional (2D) system based on the HgTe quantum well (QW) of critical width random deviations of the well width from its average value result in local crossovers from zero gap 2D Dirac fermion system to either the 2D TI or the ordinary insulator, forming a complicated in-plane network of helical channels along the zero-gap lines. We have studied experimentally the transport properties of the critical width HgTe QWs near the Dirac point, where the conductance is determined by a percolation along the zero-gap lines. The experimental results confirm the presence of percolating conducting channels of a finite width. Our work establishes the critical width HgTe QW as a promising platform for the study of the interplay between topology and localization.

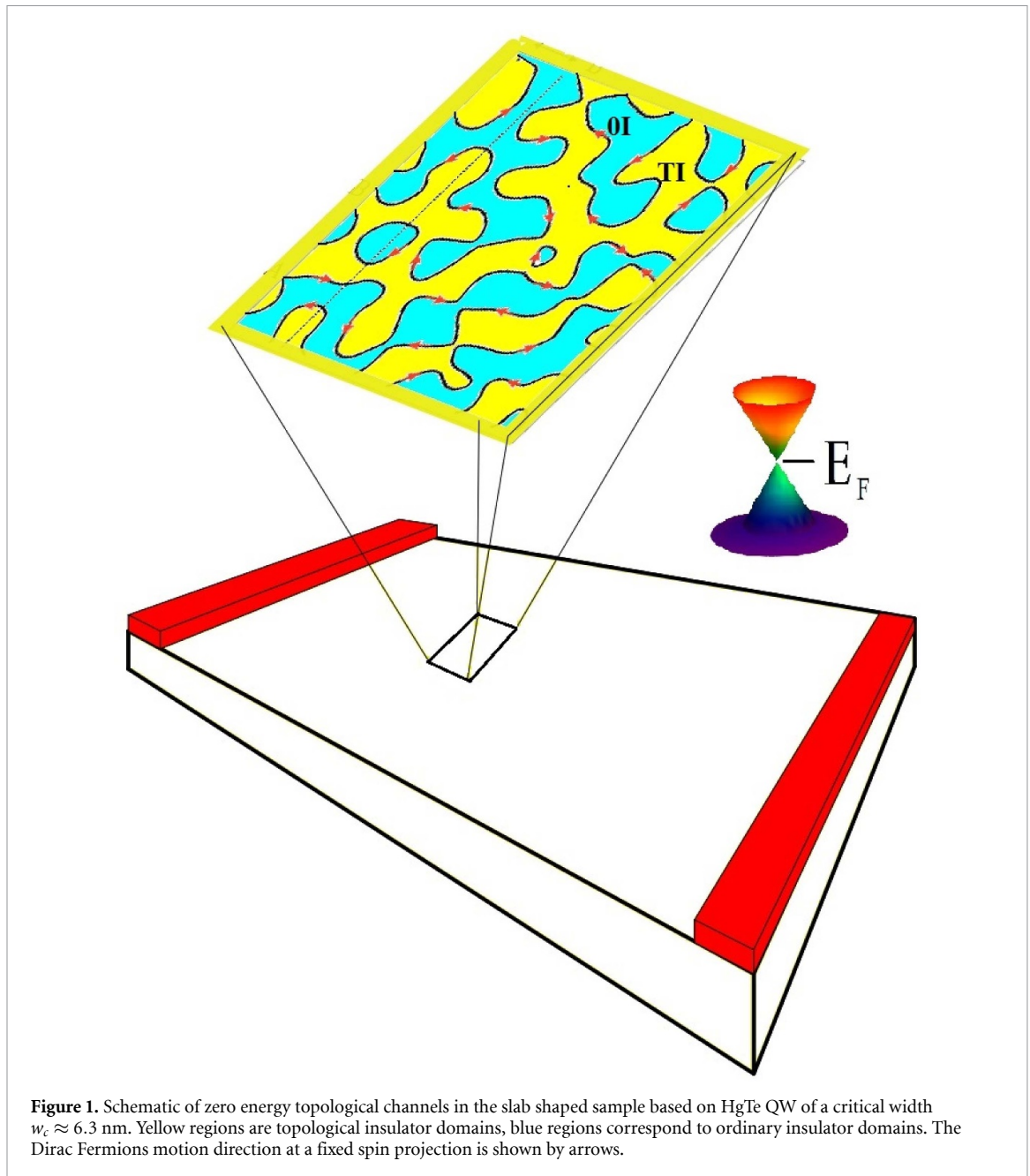
1. Introduction

Topological states of matter have attracted a lot of attention due to their numerous intriguing transport properties. In particular, in two-dimensional topological insulators (2D TIs) there are gapless conducting helical edge channels, that are protected against backscattering [1–6]. Many experiments have been performed to investigate the transport properties of the 2D TI edge states in several materials where the helical edge states are due to different physical mechanisms. For example the main factor responsible for the existence of a nontrivial topological phase in HgTe/CdTe quantum wells (QWs) is a strong spin–orbit interaction [7–12], whereas in InAs/GaSb double QWs the topologically protected helical edge states in the inverted phase emerge as a consequence of the coupling between the bands leading to the opening of a hybridization gap [13–17]. As has been verified on many occasions (for review see [18]) generally two basic experimentally observed features indicate the presence of ballistic helical edge channels in submicron 2DTI samples: the conductance of the order of the universal value e^2/h [7, 11]

and a strong nonlocal signal due to the helical edge states current circulating along the sample perimeter [9–12].

The interplay between topology and localization is another challenging object of study both for theoreticians and experimentalists. To gain a deeper insight into the critical behaviour of matter, theoreticians often employ network models. Such is the case for the metal–insulator transition and also for the transition between different phases of topological insulator (TI) [19–24]. Critical phenomena related to the integer and fractional quantum Hall effects have been successfully described by a chiral Chalker-Coddington-like network representation of bulk transport in the high magnetic field limit [25]. In contrast to the quantum Hall states, the 2D TI-metal transition could be represented by uncoupled counter propagating channels with opposite spin, the so called Z_2 network model [19, 20, 22–24, 26].

It was recognized that for topological metallic states a well-defined mobility edge, i.e. a specific energy separating the region of extended states from that of the localized states, is expected, while the extended states in quantum Hall effect are located



at particular distinct energy values (no mobility edge).

As already mentioned, a network of conducting channels occurs naturally in HgTe QWs of critical width $w_c \approx 6.3$ nm. It has been shown [7, 8, 27] that if the HgTe QW width is below the critical value, the system is an ordinary insulator (OI) with a normal energy band structure. If, on the other hand, the QW width is above the critical, then it is a 2D TI with an inverted energy spectrum. Finally, the QW width $w = w_c$ corresponds to the 2D Dirac fermion system with a gapless, single-cone spectrum (figure 1). In-plane fluctuations of the QW width about its average value $w = w_c$, that cannot be completely avoided during the QW growth, lead to spacial gap variations (random gap sign changes), and therefore, to transitions between the mentioned topological phases.

This results in a network of zero energy channels running along the boundaries separating the normal insulator and the 2D TI phases (figure 1). In addition to the gap fluctuations there will also be variations of the electrostatic potential due to random distribution of charged impurities. For the Fermi energy located near the Dirac point the system conductivity is attributed to the percolation along zero energy channels [28, 29].

In the present paper we study the transport properties of the zero gap HgTe QW (of critical width) both for $B = 0$ and in the presence of magnetic field. We find that the conductivity of the samples lies in the interval $(1.5 - 4)e^2/h$, as is expected for the topological network formed by finite width conducting channels. In order to estimate the width of the channels we performed additional measurements of

the Hall effect at low magnetic fields. Surprisingly, we find that the Hall effect near the percolation threshold is completely suppressed in a narrow interval of carrier densities in agreement with the percolation model [28, 29].

2. Results and discussion

2.1. Methods

QWs $\text{Cd}_{0.65}\text{Hg}_{0.35}\text{Te}/\text{HgTe}/\text{Cd}_{0.65}\text{Hg}_{0.35}\text{Te}$ with (013) surface orientations and a nominal well thickness of (6.3–6.6) nm were prepared by molecular beam epitaxy (see figures 2 and 3). As shown in the previous publications [10], the use of substrates inclined to the singular orientations facilitates the growth of more perfect films. Therefore, the growth of alloys is performed predominantly on the substrates with surface orientation [013], which deviates from the singular orientation by approximately 19° . Fabrication of ohmic contact to HgTe QW is similar to that for other 2D systems, such as GaAs QWs, for example: the contacts were formed by the burning-in of indium directly on the surface of large contact pads. Modulation-doped HgTe/CdHgTe QWs are typically grown at 180°C , which is relatively low compared to III–V compounds. On each contact pad the indium diffuses vertically down, providing ohmic contact to the underlying QW, with the contact resistance in the range of 0.1–1 kOhm. During the AC measurements we made sure that the Y-component of the impedance did not exceed 5% of the total impedance, which is the indication of good ohmicity of the contacts. The sample is a Hall bar device with eight voltage probes. The bar has the width W of $50\ \mu\text{m}$ and three consecutive segments of different lengths L (100, 250, $100\ \mu\text{m}$) (figure 3, left bottom panel). A dielectric layer was deposited (100 nm of SiO_2 and 100 nm of Si_3Ni_4) on the sample surface and then covered by a TiAu gate. The density variation with gate voltage was $1 \times 10^{11}\ \text{cm}^{-2}\ \text{V}^{-1}$. The magnetotransport measurements were performed in the temperature 4.2 K using a standard four point circuit with a 1–13 Hz ac current of 1–10 nA through the sample, which is sufficiently low to avoid overheating effects.

2.2. Structural properties

Transmission electron microscopy (TEM) of cross sectional sample allows to study the interfaces of layered structures directly with a spatial resolution down to an nanometer scale. Figure 2(a) shows TEM images of the cross sections of the specimen with designations of various layers constituting the structures, which allow assessment of abruptness of interfaces as well as lateral uniformity of layer growth [30]. The difference of contrasts in TEM images is due to the difference in the chemical compositions of the layers, which allows to determine the fluctuation of the width of the individual layers in the image of a multilayer structure. Both images indicate that

HgTe/HgCdTe interfaces are reasonably abrupt. A histogram in figure 2(b) is a display of statistical information on HgTe well width fluctuations. The histogram follows a normal Gaussian distribution with mean with $d = w_c \approx 6.1\ \text{nm}$ with standard deviation of 0.6 nm. As we mentioned above, the width fluctuations near topological transition lead to spacial gap variations, and therefore, to transitions between the topological phases.

Independently the QW thickness has been controlled by *in situ* ellipsometric method [31]. The accuracy was $\pm 0.5\ \text{nm}$ in determining the thickness, which agrees with TEM measurements. Note, however, that this method demonstrate only average parameters of the well fluctuation, while TEM image allows to deduce spatial resolution of the well fluctuations.

2.3. Gapless Dirac fermions and Drude conductivity

Recently it has been demonstrated that HgTe QW with a critical width $w_c = 6.3\ \text{nm}$ constitutes a system of 2D fermions with a single Dirac cone spectrum [27, 32–34]. The fluctuations of the QW width result in a random potential in the bulk of the QW. In QW of critical width these fluctuations lead to the formation of a random network of zero energy lines, as shown in figure 1. We believe that the physical properties of this network are described by Z_2 quantum network model, and below we present experimental evidence that supports this assumption.

Devices for transport measurements (see chapter method) are specially designed for multi-terminal measurements and consists of three narrow ($50\ \mu\text{m}$ wide) consecutive segments of different length (100, 250, $100\ \mu\text{m}$) and seven voltage probes (see figure 3, left bottom panel). A dielectric layer was deposited (100 nm of SiO_2 and 100 nm of Si_3Ni_4) on the sample surface and then covered by a TiAu gate (see figure 3, left top panel). In conventional transport measurements the current is applied between contacts 1–6 and the potential difference is measured between contacts 2–3, 3–4 and 4–5 of the sample. Figure 3 shows the resistivity $\rho(V_g)$ at zero magnetic field for five samples fabricated from different wafers and at different time. The table 1 lists the typical parameters of the devices, such as the well width w , the gate voltage corresponding to the Dirac point position V_{CNP} , the resistivity value at the CNP ρ_{max} and the electron mobility $\mu = \sigma/n_s e$ for the density $n_s = 10^{11}\ \text{cm}^{-2}$. The figure 4(a) shows the conductivity distribution for 24 samples, grown during a five years period. One can see that the conductivity values lie in the interval $(1.5 - 4)e^2/h$. Figure 4(b) shows the conductivity as a function of gate voltage V_g for five representative samples with parameters listed in table 1. The $\sigma(V_g)$ dependence is symmetric and nearly parabolic close to the CNP for low electron densities ($n_s < 2 \times 10^{10}\ \text{cm}^{-2}$) and approximately linear in electron density for higher

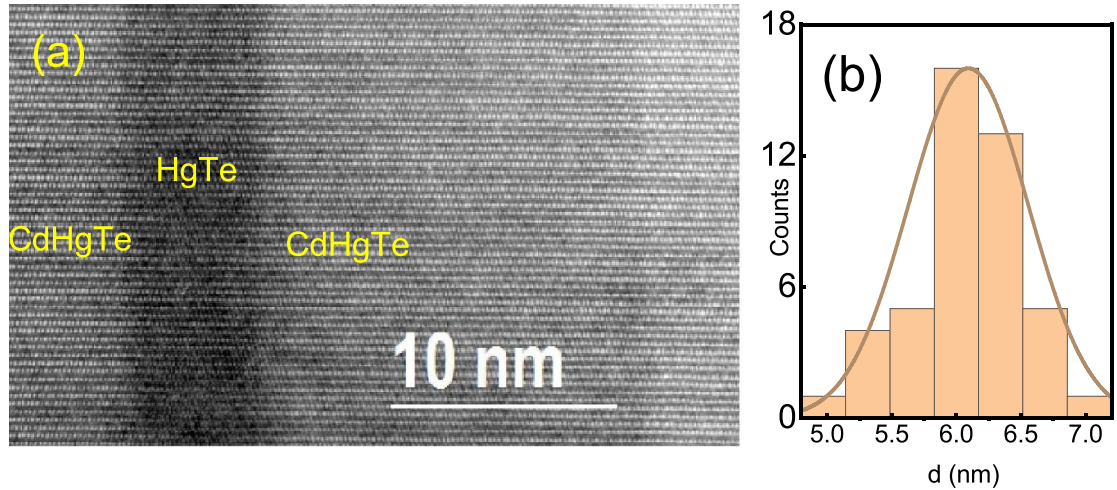


Figure 2. (a) TEM images of cross sections of sample. (b) Histogram displaying the distribution of well widths across the whole image.

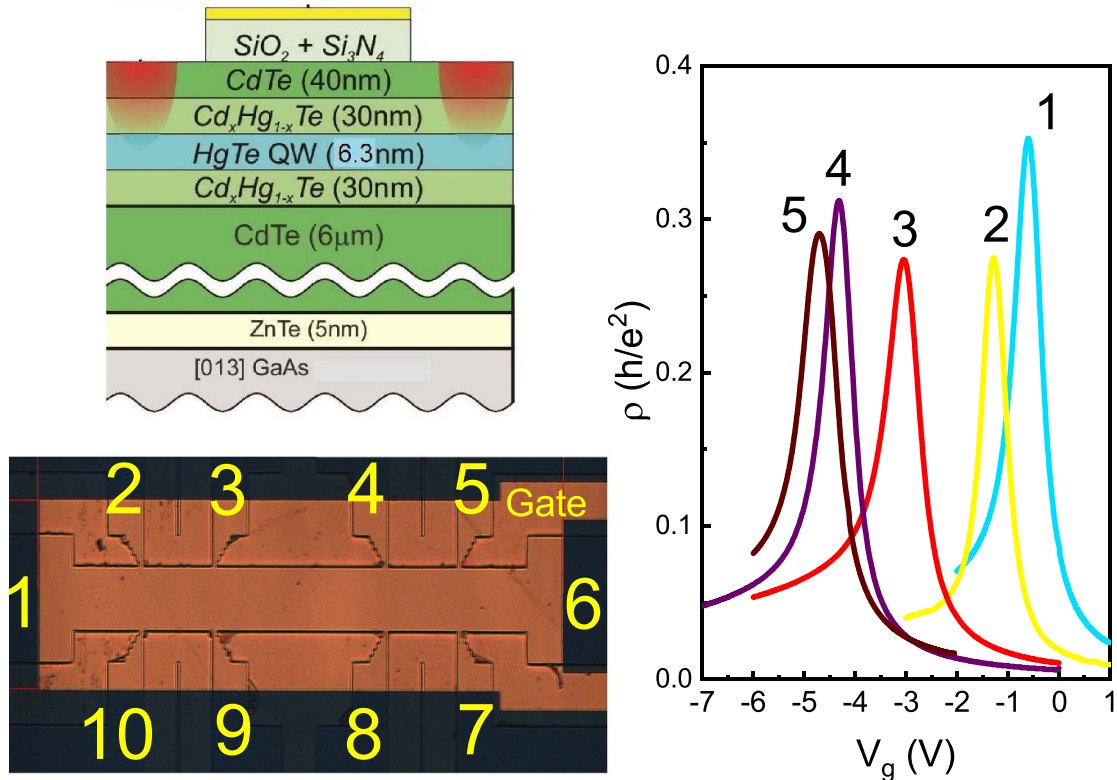


Figure 3. Resistance as a function of the gate voltage for different samples, $T = 4.2$ K. Left top—schematic structure of the sample. Left bottom—top view of the sample.

Table 1. Some of the typical parameters of the electron system in HgTe QW at $T = 4.2$ K.

Sample	w (nm)	V_{CNP} (V)	ρ_{max} (h/e^2)	μ ($V\text{ cm}^{-2}\text{ s}^{-1}$)
1	6,3	-0.6	0.35	56.000
2	6,4	-1.28	0.27	90.000
3	6,3	-3	0.27	59.600
4	6,3	-4.3	0.31	58.600
5	6,3	-4.7	0.29	46.400

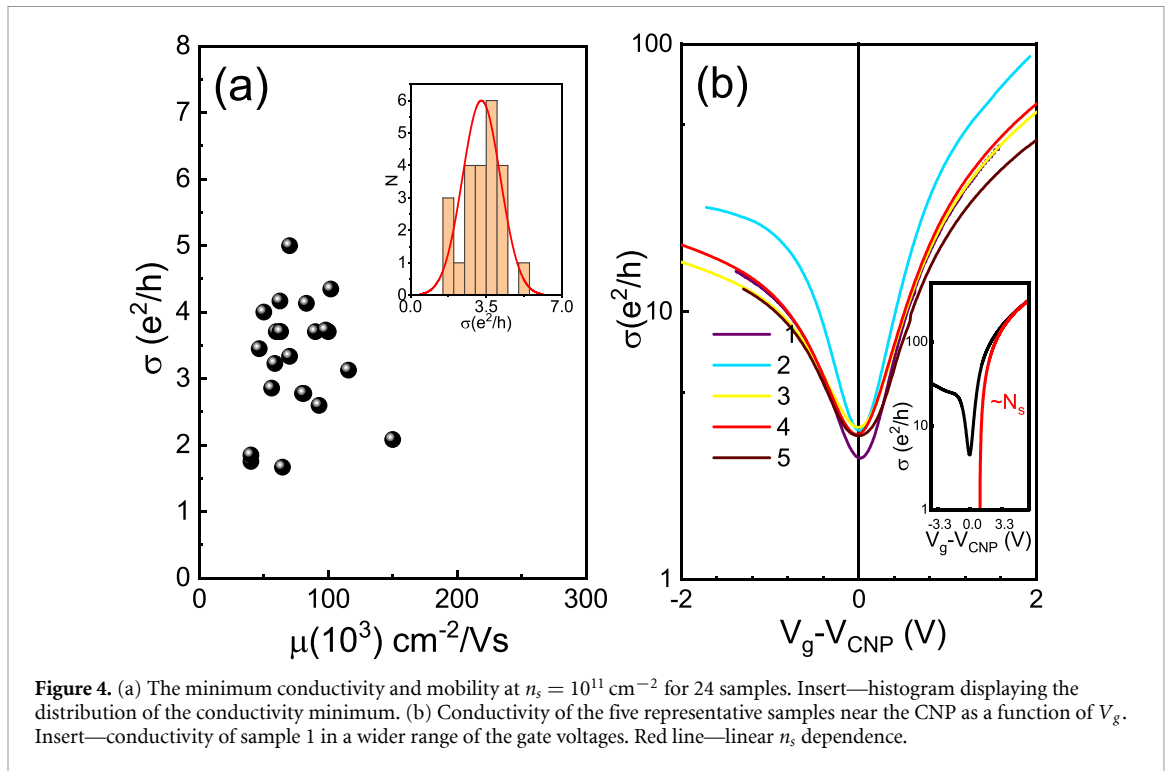


Figure 4. (a) The minimum conductivity and mobility at $n_s = 10^{11} \text{ cm}^{-2}$ for 24 samples. Insert—histogram displaying the distribution of the conductivity minimum. (b) Conductivity of the five representative samples near the CNP as a function of V_g . Insert—conductivity of sample 1 in a wider range of the gate voltages. Red line—linear n_s dependence.

density values. It is convenient to consider the total conductivity as a sum of the network conductivity σ_{mw} and the bulk conductivity σ_{2D} : $\sigma_{tot} = \sigma_{mw} + \sigma_{2D}$.

Let us start our analysis with the bulk contribution to the conductivity. The unscreened Coulomb disorder induced by randomly distributed charge impurities has been considered as the dominant mechanism of scattering in HgTe QW because of a very large HgTe dielectric constant and small Dirac fermions effective mass. Two distinct transport regimes can be indicated. For large carrier density the Boltzmann transport theory is valid [35]. On approaching the Dirac point (low carrier density), at a certain energy there will be an Anderson transition from the higher energy delocalized states to the localized states in narrow impurity bands located in small direct or inverted energy gaps [28]. It means that the 2D bulk conductivity inside these gaps is much less than e^2/h or $k_F \ll 1$, where k_F is the Fermi vector. In this situation the localization length is equal to the mean free path l [36] and electrons are strongly localized. Strictly speaking in a 2D case all states are supposed to be localized at zero T and for infinite sample. However, transition from metallic-like to insulator behaviour can be observed due to interaction effects [37]. Moreover, spin orbit interaction does not suppress strong localization in the limit $k_F \ll 1$, while in the metallic limit weak antilocalization is observed (see for example [38]).

It would be reasonable to suppose that transport via the delocalized states near the boundary with the localized bands can be described using the ordinary expression for mobility of carriers with a parabolic spectrum in the presence of impurity scattering. In

this case the mobility is given by $\mu = A(n_s/n_i)$, where n_i is the impurity density, $A = (\epsilon_s/e^3)(16\pi\hbar^3/m_{DF}^2)$, m_{DF} is the effective mass at the Fermi level [39]. We get $\sigma_{2D} = e\mu n_s$ with quadratic dependence on electron density for $n_s < 2 \times 10^{10} \text{ cm}^{-2}$, as shown in figure 4(b). At higher electron densities the electron energy spectrum becomes linear and one has to use the transport time expression calculated in [35], which leads to a conductivity $\sigma(n_s)$ nearly linear with the electron density. Such conductivity behaviour is shown in figure 4(b). The gap fluctuations due to roughness may lead to the additional scattering far from the charge neutrality point. This non-trivial mechanism of the scattering is considered in paper [35].

2.4. Comparison with the network model

Transport in HgTe QWs of a critical width w_c is believed to be governed by the energy gap fluctuations leading to the formation of the topological channels network (figure 1). One can assume that the QW width fluctuations δw can be described by the Gaussian distribution around the medium width value w , which follows from TEM images of the sample (figure 2).

The percolation network can be characterized by a dimensionless parameter $\xi = \text{erfc}((w - w_c)/\sqrt{2}\delta w)$, where $\text{erfc}(x)$ is the complementary error function. The unavoidable QW width fluctuations lead to a sample breaking-up into domains with positive (the OI) and negative (the TI) gap signs. If $|w - w_c| \gg \delta w$ and $w > w_c$ ($\xi \rightarrow 1$), then rare OI domains are embedded in TI domains. If, on the other hand, $w < w_c$, $\xi \rightarrow 1$, then rare TI domains are embedded in OI

domains. For $w \rightarrow w_c$ ($\xi \rightarrow \xi_c = 0.5$) these domains are mixed in approximately equal proportion.

At the CNP the low-temperature the bulk conductivity of the OI or the TI domains should be close to zero. However, in the immediate vicinity of the lines separating the OI and TI domains (the zero gap line (ZGL)) the QW is a nearly gapless conductor. In fact, any such ZGL can be considered as a quantum wire. The sample conductance will be non-zero if such a line runs from one end of the sample to the other. On approaching the percolation threshold there forms a whole network of ZGLs covering the entire sample.

If the gap fluctuations are smooth, the wire associated with the ZGL will have many 1D subbands occupied. The important point is that two of these subbands will be the Weil states with a linear dispersion topologically protected from electron backscattering. The Weil states are similar to the edge states in Bernevig–Hughes–Zhang model of the 2D TI edge. In a small ballistic sample the edge state yields a dissipationless conductance equal to the conductance quantum.

In a large random system with a size exceeding the QW width fluctuation correlation length the ZGLs form a dense network. In this case the 2D conductivity is a combination of the ideal conductance of a Weil state and the conductance associated with tunnelling between different ZGLs lying close to each other.

The hopping between the ZGLs is realized via intermediate Dirac states, which lowers the hopping energy (as compared to the total gap) and raises the hopping probability amplitude. In any case one can use the characteristic hopping length between different ZGLs as some given quantity. Our consideration is based on geometric fractal properties of ZGLs.

We suppose that in our sample $|\xi - \xi_c| \ll 1$ so that a network of OI and TI domains is formed and the ZGLs cover the entire sample. It is worth noting, however, that in a realistic random network of channels a low temperature non-zero 2D conductivity may occur only if electrons can tunnel between the adjacent channels, for which a finite channel width is required [29]. One can estimate that:

$$\frac{|w - w_c|}{w_c} \sim \left(\frac{\hbar v}{\alpha a w_c} \right)^r \quad (1)$$

where $\alpha = \partial \Delta(w) / \partial w|_{w=w_c}$, Δ is the rms energy gap fluctuation value, v is the electron velocity, r is parameter, which is close to 0.45 [29]. The conductivity of the network can be estimated from the equation [29]:

$$\sigma = \frac{e^2 D}{2\pi \hbar^2 v a} \sim \frac{e^2}{h} \left(\frac{\Delta a}{\hbar v} \right)^p \quad (2)$$

where $D \simeq av(\Delta a / \hbar v)^p$ is the diffusion coefficient, p is a coefficient close to 0.15. We estimate the corresponding HgTe QW parameters from

[29]: $\hbar v = 560$ meV; $\alpha \approx -8.75$ meV nm⁻¹, $\Delta \approx |\alpha| \sqrt{w^2 - \bar{w}^2} \approx 4$ meV, $a = 30$ nm.

Combining all parameters we obtain $\sigma(n_w) = (e^2/h)(1 \pm 0.1)$, which is smaller than the average experimental value $\sigma_{\text{exp}} = (e^2/h)(2.5 \pm 1)$. This disagreement can be diminished if one takes into account the edge states nonzero width. This results in new percolation paths and, correspondingly, in higher σ_{nw} values and also in a much stronger σ_{nw} dispersion in agreement with the experiment.

The percolation model [29] predicts a non-zero conductivity in a narrow width interval near the critical value w_c due to the suppression of backscattering of electrons propagating along ZGLs and the growing hopping between adjacent ZGLs as $\bar{w} \rightarrow w_c$. It is expected, that the network conductivity vanishes outside of this percolation threshold. One can estimate the energy and the charge density interval where percolation conductivity occurs. However, in the experiment the total conductivity does not show a crossover from $\sim e^2/h$ values to zero beyond the percolation threshold, expected from the network model. Instead we observe a smooth conductivity growth with density near the CNP (figures 3 and 4(b)). As we already discussed above, the percolation conductivity is short-circuited by the conductivity of the bulk electrons.

It would be instructive to compare results for the minimum conductivity with the theoretical predictions for other two-dimensional Dirac materials, such as graphene (see for example [40]). The universal result predicted by many theoretical models is $\sigma = 2e^2/(\pi h)$ per valley for the case of the ideal crystal and in the presence of weakly scattering impurities [41, 42]. This prediction disagrees with the experimentally observed minimum conductivity in graphene samples, which is found to be much larger and sample dependent. The experimental results [43] provide convincing evidence, that long-range scatterers such as charged impurities induce spatial inhomogeneities of the carrier density that, result in the formation of electron hole puddles ([40]). Therefore electrical conductivity near Dirac point in realistic graphene devices is described by disorder-induced carrier density inhomogeneity in contrast to HgTe well, where disorder is related to the well width fluctuations. We can not fully discriminate this prediction from the percolation model, therefore we have to consider additional arguments, such as the observation of the well width fluctuations, mentioned above, and the zeroth Hall effect, which we consider below.

2.5. The Hall effect in topological channel system

The percolation model also predicts other characteristic peculiarities in the transport coefficients behaviour as well. One of the key effects proving the presence of a network structure in the system studied is the quenching of the Hall effect at low magnetic field.

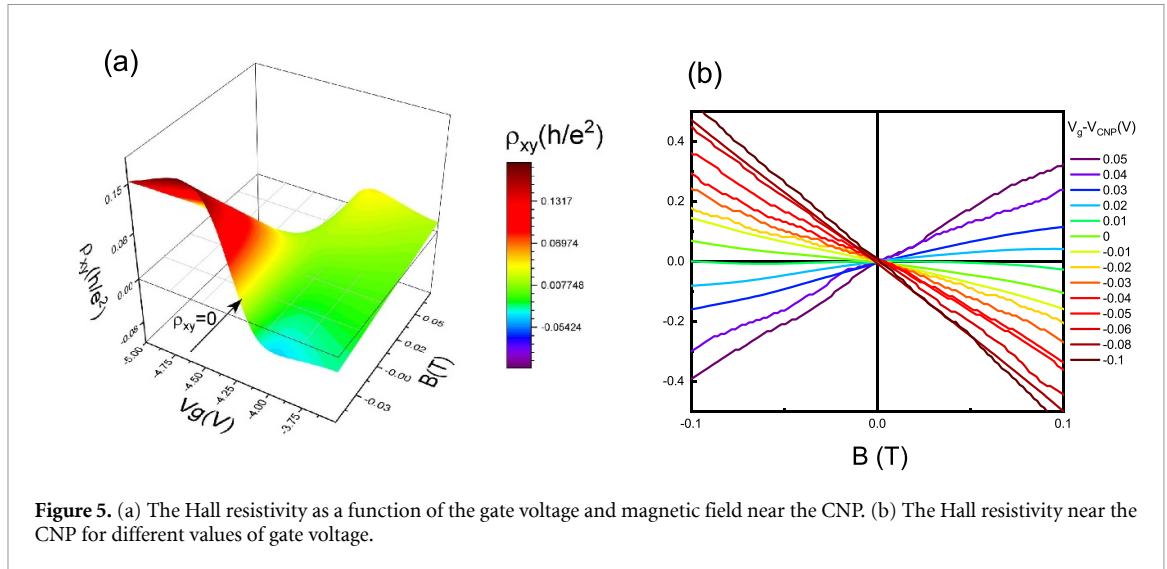


Figure 5. (a) The Hall resistivity as a function of the gate voltage and magnetic field near the CNP. (b) The Hall resistivity near the CNP for different values of gate voltage.

The figures 5(a) and (b) show the Hall resistivity as a function of gate voltage and magnetic field. Figure 5(b) shows a number of representative $\rho_{xy}(B)$ curves for $V_g = V_{CNP}$, $V_g < V_{CNP}$ and $V_g > V_{CNP}$. One can see a very narrow $\Delta V_g \simeq 0.05 V$ region near the CNP, where $\rho_{xy} \approx 0$. Figures 5(a) and (b) show that the Hall resistivity is flat and close to zero in the interval of magnetic field $-0.1 T < B < 0.1 T$. So, according to experiment there is a quenching of the Hall effect at the CNP in the energy interval corresponding to the density variation $\delta n_s \sim 5 \times 10^9 \text{ cm}^{-2}$.

From the theoretical point of view one can treat this situation as follows. A curved 1D ZGL state can be mapped on the QW plane using the coordinate $\mathbf{r}(s)$, where s is the length along the edge and $\mathbf{s} = d\mathbf{r}(s)/ds$ is the tangent to the curve. If we take the magnetic field $\mathbf{B} = (0, 0, B)$ and the corresponding vector potential $\mathbf{A} = \mathbf{B} \times \mathbf{s}$ then the Hamiltonian of an electron in the 1D ZGL state will be $H = \sigma \nu_F (p - e[\mathbf{B} \times \mathbf{r}(s)]s/c)$, where σ is a spin index and ν_F is the Fermi velocity. The gauge transform $U = \exp(i(e/c) \int [\mathbf{B} \times \mathbf{r}(s)] ds)$ converts the Hamiltonian H to σp . In this way, as one can see, the magnetic field can be effectively eliminated from the Hamiltonian for all open-ended ZDLs which define the character of the low-temperature transport. And this cancels the Hall current as well. Indeed, the above gauge transform shows that the effect of magnetic field on such a system will be null unless the ZGL are closed or are not single-connected. But in general the ZGL do not branch out. In fact, the presence of a branching point (x_0, y_0) means a simultaneous fulfillment of three conditions: $\Delta(x_0, y_0) = 0$, $\partial_{x_0}(x_0, y_0) = 0$ and $\partial_{y_0}(x_0, y_0) = 0$, which is practically impossible. Hence, the theory predicts a zero Hall current in the presence of magnetic field, in agreement with the experimental.

It worth noting that the bulk contribution to the Hall current will also be absent. Indeed, under these

conditions the Fermi energy will be located in a narrow band of localized states. One can estimate this band width δ_b from the density interval $\delta n_s = 5 \times 10^9 \text{ cm}^{-2}$ corresponding to the quenching of the Hall effect (see above). Using the value of DoS obtained from capacitance measurements [44] yields $\delta_b = 3 \text{ meV}$. This estimate means that the band width of localized states is close to the characteristic disorder amplitude in HgTe QW.

3. Summary and conclusion

In conclusion, our results provide an opportunity to take a fresh look at the nature of electron transport in HgTe QWs of critical thickness. The description of transport in this system in terms of percolation through a network of one-dimensional conducting channels makes it possible to study the effects caused by the interplay of topology and localization. More generally, the study of transport in zero gap HgTe QWs can improve our understanding of the disorder induced TI-to-metal transition and may be important for a wider class of disordered 2D electron systems, than was considered previously.


Data availability statement

The data that support the findings of this study are available upon reasonable request from the authors.

Acknowledgment

G M Gusev acknowledges for financial support FAPESP (Brazil) and CNPq (Brazil); Z D Kvon, D A Kozlov, E B Olshanetsky, M V Entin and N N Mikhailov acknowledge for financial support Ministry of Science and Higher Education of the Russian Federation, Grant No. 075-15-2020-797(13.1902.21.0024).

ORCID iD

G M Gusev  <https://orcid.org/0000-0003-3646-6024>

References

- [1] Kane C L and Mele E J Z 2005 Topological order and the quantum spin Hall effect *Phys. Rev. Lett.* **95** 146802
- [2] Hasan M Z and Kane C L 2010 Topological insulator *Rev. Mod. Phys.* **82** 2045
- [3] Qi X-L and Zhang S-C 2011 Topological insulators and superconductors *Rev. Mod. Phys.* **83** 1057
- [4] Qi X-L and Zhang S-C 2010 The quantum spin Hall effect and topological insulators *Phys. Today* **63** 33
- [5] Moore J E and Balents L 2007 Topological invariants of time-reversal-invariant band structures *Phys. Rev. B* **75** 121306
- [6] Moore J E 2010 The birth of topological insulators *Nature* **464** 194
- [7] König M, Wiedmann S, Brune C, Roth A, Buhmann H, Molenkamp L W, Qi X-L and Zhang S-C 2007 Quantum spin Hall insulator state in HgTe quantum *Science* **318** 766
- [8] Buhmann H 2011 The quantum spin Hall effect *J. Appl. Phys.* **109** 102409
- [9] Roth A, Brüne C, Buhmann H, Molenkamp L W, Maciejko J, Qi X-L and Zhang S-C 2009 Nonlocal transport in the quantum spin Hall state *Science* **325** 294
- [10] Gusev G M, Kvon Z D, Shegai O A, Mikhailov N N, Dvoretzky S A and Portal J C 2011 Transport in disordered two-dimensional topological insulators *Phys. Rev. B* **84** 121302(R)
- [11] Olshanetsky E B, Kvon Z D, Gusev G M, Levin A D, Raichev O E, Mikhailov N N and Dvoretzky S A 2015 Persistence of a two-dimensional topological insulator state in wide HgTe quantum wells *Phys. Rev. Lett.* **114** 126802
- [12] Rahim A, Levin A D, Gusev G M, Kvon Z D, Olshanetsky E B, Mikhailov N N and Dvoretzky S A 2015 Scaling of local and nonlocal resistances in a 2D topological insulator based on HgTe quantum well *2D Mater.* **2** 044015
- [13] Knez I, Du R-R and Sullivan G 2011 Evidence for helical edge modes in inverted InAs/GaSb quantum wells *Phys. Rev. Lett.* **107** 136603
- [14] Knez I, Rettner C T, Yang S-H, Parkin S S P, Du L, Du R-R and Sullivan G 2014 Observation of edge transport in the disordered regime of topologically insulating InAs/GaSb quantum wells *Phys. Rev. Lett.* **112** 026602
- [15] Du L, Knez I, Sullivan G and Du R-R 2015 Robust helical edge transport in gated InAs/GaSb bilayers *Phys. Rev. Lett.* **114** 096802
- [16] Nichele F, Pal A N, Pietsch P, Ihn T, Ensslin K, Charpentier C and Wegscheider W 2014 Insulating state and giant nonlocal response in an InAs/GaSb quantum well in the quantum Hall regime *Phys. Rev. Lett.* **112** 036802
- [17] Suzuki K, Harada Y, Onomitsu K and Muraki K 2015 Gate-controlled semimetal-topological insulator transition in an InAs/GaSb heterostructure *Phys. Rev. B* **91** 245309
- [18] Bernevig B A 2013 *Topological Insulators and Topological Superconductors* (Princeton, NJ: Princeton University Press)
- [19] Onoda M, Avishai Y and Nagaosa N 2007 Localization in a quantum spin Hall system *Phys. Rev. Lett.* **98** 076802
- [20] Obuse H, Furusaki A, Ryu S and Mudry C 2007 Two-dimensional spin-filtered chiral network model for the Z₂ quantum spin-Hall effect *Phys. Rev. B* **76** 075301
- [21] Obuse H, Furusaki A, Ryu S and Mudry C 2008 Boundary criticality at the Anderson transition between a metal and a quantum spin Hall insulator in two dimensions *Phys. Rev. B* **78** 115301
- [22] Bondesan R, Gruzberg I A, Jacobsen J L, Obuse H and Saleur H 2012 Exact exponents for the spin quantum Hall transition in the presence of multiple edge channels *Phys. Rev. Lett.* **108** 126801
- [23] Yamakage A, Nomura K, Imura K-I and Kuramoto Y 2013 Criticality of the metal-topological insulator transition driven by disorder *Phys. Rev. B* **87** 205141
- [24] Bhardwaj S, Mkhitarian V V and Gruzberg I A 2014 Supersymmetry approach to delocalization transitions in a network model of the weak-field quantum Hall effect and related models *Phys. Rev. B* **89** 235305
- [25] Chalker J T and Coddington P D 1988 Percolation, quantum tunnelling and the integer Hall effect *J. Phys. C: Solid State Phys.* **21** 2665
- [26] Li J, Chu R-L, Jain J K and Shen S-Q 2009 Topological Anderson insulator *Phys. Rev. Lett.* **102** 136806
- [27] Buttner B et al 2011 Single valley Dirac fermions in zero-gap HgTe quantum wells *Nat. Phys.* **7** 418
- [28] Mahmoodian M M and Entin M V 2019 Microwave absorption in 2D topological insulators with a developed edge states network *Phys. Status Solidi b* **256** 1800652
- [29] Mahmoodian M M and Entin M V 2020 Conductivity of a two-dimensional HgTe layer near the critical width: the role of developed edge states network and random mixture of p- and n-domains *Phys. Rev. B* **101** 125415
- [30] Yahniuk I et al 2019 Magneto-transport in inverted HgTe quantum wells *npj Quantum Mater.* **4** 13
- [31] Dvoretzky S A, Ikusov D G, Kh. K D, Mikhailov N N, Dai N, Smirnov R N, Sidorov Y G and Shvets V A 2007 Growing HgTe Cd Hg Te 0.735 0.265 quantum wells by molecular beam epitaxy *Optoelectron. Instrument. Proc.* **43** 375
- [32] Kozlov D A, Kvon Z D, Mikhailov N N and Dvoretzky S A 2012 Weak localization of Dirac fermions in HgTe quantum wells *JETP Lett.* **96** 730
- [33] Kozlov D A, Kvon Z D, Mikhailov N N and Dvoretzky S A 2014 Quantum Hall effect in a system of gapless Dirac fermions in HgTe quantum wells *JETP Lett.* **100** 724
- [34] Gusev G M, Kozlov D A, Levin A D, Kvon Z D, Mikhailov N N and Dvoretzky S A 2017 Robust helical edge transport at $\nu = 0$ quantum Hall state *Phys. Rev. B* **96** 045304
- [35] Dobretsova A A, Kvon Z D, Braginskii L S, Entin M V and Mikhailov N N 2016 Mobility of Dirac electrons in HgTe quantum wells *JETP Lett.* **104** 388
- [36] Lee Patrick A and Ramakrishnan T V 1985 Disordered electronic systems *Rev. Mod. Phys.* **57** 287
- [37] Abrahams E, Kravchenko S V and Sarachik M P 2001 Metallic behavior and related phenomena in two dimensions *Rev. Mod. Phys.* **73** 251
- [38] Gantmakher V F 2005 *Electrons and Disorder in Solids* (Oxford: Oxford University Press)
- [39] Davies J 1997 *The Physics of Low Dimensional Semiconductors* (Cambridge: Cambridge University Press)
- [40] Das Sarma S, Adam Shaffique H E Rossi Enrico H 2011 Electronic transport in two-dimensional graphene *Rev. Mod. Phys.* **83** 407
- [41] Ostrovsky P M, Gornyi I V and Mirlin A D 2006 Electron transport in disordered graphene *Phys. Rev. B* **74** 235443
- [42] Katsnelson M I 2006 Zitterbewegung, chirality and minimal conductivity in graphene *Eur. Phys. J. B* **51** 157
- [43] Jang C, Adam S, Chen J-H, Williams E D, Sarma S D and Fuhrer M S 2008 Tuning the effective fine structure constant in graphene: opposing effects of dielectric screening on short- and long-range potential scattering *Phys. Rev. Lett.* **101** 146805
- [44] Kozlov D A, Savchenko M L, Ziegler J, Kvon Z D, Mikhailov N N, Dvoretzky S A and Weiss D 2016 Capacitance spectroscopy of a system of gapless Dirac fermions in a HgTe quantum well *JETP Lett.* **104** 859